Regional Studies in Marine Science 90 (2025) 104451

Contents lists available at ScienceDirect

Regional Studies in Marine Science

journal homepage: www.elsevier.com/locate/rsma

Spatial distribution of extreme upwelling event in the Seas of Alor Kecil, Indonesia, revealed by UAV's thermal infrared sensor

Anindya Wirasatriya [a,b,*], Sigit Bayhu Iryanthony [b], R. Dwi Susanto [a,c], Teguh Agustiadi [d], Kunarso [a], Aris Ismanto [a], Muhammad Helmi [a,b], Muhammad Zainuri [a], Rikha Widiaratih [a], Gentio Harsono [e,f], Dwiyoga Nugroho [d], Adi Purwandana [d], Shoimatul Fitria [g], Jahved Ferianto Maro [h], Yupiter Nungnulang Sondy Kitarake [i], Efrin Antonia Dollu [h], Riandi Teguh Widiyandono [b], Chunhua Qiu [j,k], Anjar Dimara Sakti [l], Priyadi Dwi Santoso [m], Elifelet Kelendonu [n]

[a] Department of Oceanography, Faculty of Fisheries and Marine Science, Universitas Diponegoro, Tembalang Campus, St. Prof. Jacub Rais, Semarang, Central Java, Indonesia
[b] Center for Coastal Rehabilitation and Disaster Mitigation Studies, Universitas Diponegoro. Jl. Prof. H. Soedarto, S.H., Tembalang Campus, Semarang, Central Java 50275, Indonesia
[c] Dept. of Atmospheric and Oceanic Science, University of Maryland, College Park, MD 20742, USA
[d] Research Center for Oceanography, National Research and Innovation Agency, Jakarta, Indonesia
[e] Faculty of Science and Defense Technology, Republic of Indonesia Defense University, Indonesia
[f] Hidro-Oceanographic Center, Indonesian Navy Jl. Pantai Kuta V No. 1, Jakarta, Indonesia
[g] Dep. of Management, Faculty of Economics and Business, Diponegoro University, Indonesia
[h] Dept. of Fisheries, Faculty of Agriculture and Fisheries, Universitas Tribuana Kalabahi, Alor, Indonesia
[i] Marine and Fisheries Agency of Alor Regency, Indonesia
[j] School of Marine Sciences, Sun Yat-sen University, and Southern Marine Science and Engineering Guangdong Laboratory (Zhuhai), Zhuhai, China
[k] Guangdong Provincial Key Laboratory of Marine Resources and Coastal Engineering, School of Marine Sciences, Sun Yat-sen University, Guangzhou, 510275, China
[l] Geographic Information Sciences and Technology Research Group, Faculty of Earth Sciences and Technology, Institut Teknologi Bandung, Bandung, Indonesia
[m] Research Center for Deep Sea, National Agency for Research and Innovation, Jakarta, Indonesia
[n] Tourism Agency of Alor Regency, Indonesia

ARTICLE INFO

Keywords:
Extreme upwelling
Alor island
Thermal infrared senSor
Unmanned aerial vehicle (UAV)
Indonesian throughflow (ITF)

ABSTRACT

Dramatic and quick drop in sea surface temperature (SST) of more than 10°C is what distinguishes an extreme upwelling event (EUE) in the seas of Alor Kecil, Alor Island, Indonesia. The minimum SST due to extreme upwelling can reach 12°C, making this the sole phenomenon in the world because no tropical seas have such cold SST. EUE occurs solely along the Mulut Kumbang Strait, which is 300 m wide and 900 m long. This phenomenon only occurs at spring tides from August to November, lasting about one hour each time. We were able to expose detailed characteristics of SST distribution throughout the peak and fading stages of EUE from 1 to 4 September 2023 using thermal infrared sensors placed on the Unmanned Aerial Vehicle. During EUE, the SST distribution also reveals the complex current pattern distribution. The minimum SST during the peak of EUE is 12°C. Northward flood current brings cold water from the deeper layer in front of the strait mouth into the strait, where it meets the southward background current, which is probably related to Indonesian Throughflow (ITF), forming a strong SST front in the strait's northern portion. The SST differential between two water masses in the front area exceeds 5°C, making this one of the strongest SST fronts in the world. The flood current also transports warm surface water from the Pantar Strait, creating warm water plume among the relatively cold water masses within the strait. During EUE decay, combined ebb and background currents generate a strong, warmed southerly current that drives cold water back to the deep layer in front of the strait mouth. This study indicates

* Corresponding author at: Department of Oceanography, Faculty of Fisheries and Marine Science, Universitas Diponegoro, Tembalang Campus, St. Prof. Jacub Rais, Semarang, Central Java, Indonesia.
E-mail address: anindyawirasatriya@lecturer.undip.ac.id (A. Wirasatriya).

https://doi.org/10.1016/j.rsma.2025.104451
Received 12 October 2024; Received in revised form 17 May 2025; Accepted 25 August 2025
Available online 27 August 2025

the new insight of the interaction between the global scale circulation as represented by ITF and local scale tidal current that generate EUE in the seas of Alor Kecil.

1. Introduction

Upwelling refers to the process of rising water masses from deeper water columns to the surface over a relatively long period of time (several days to several weeks) so that it is able to lift the water masses in a vertical distance of 100 m or more (Kämpf and Chapman, 2016). The mechanism of coastal upwelling involves the role of surface wind blowing along the coastline that generates offshore Ekman transport. This process brings cold water masses to the sea surface that reduces sea surface temperature (SST) by 2–4° along the coastal line (e.g.,

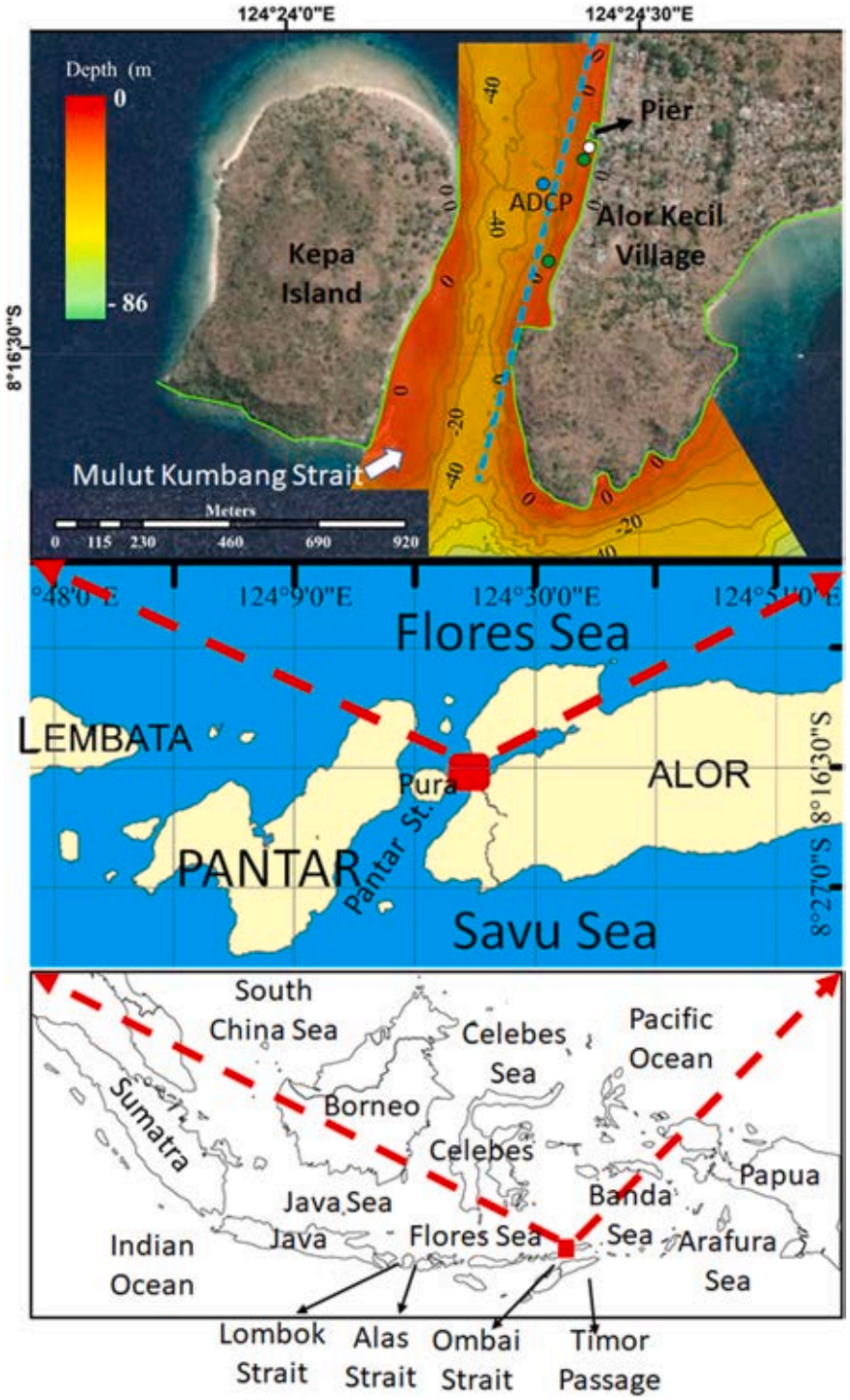

Fig. 1. Mulut Kumbang Strait; the location of the Extreme Upwelling Event. The blue dashed line denotes the UAV's flying track. Green, white, and blue dots denote the positions of the temperature loggers, tide logger, and ADCP, respectively. Bathymetry data was taken from single- beam echosounder described in Wirasatriya et al. (2023).

Table 1
Specification of cameras mounted on the Mavic 2 Enterprise Advanced.

Specification	Description
Thermal Infrared (TIR) Camera	
Sensor	Uncooled VOx Microbolometer
Focal Length	Approx. 9 mm; 35 mm format equivalent: Approx. 38 mm
Sensor Resolution	640 × 512 @30 Hz
Accuracy of Thermal Temperature	Measurement: ±2℃ or ±2 %, whichever is greater.
Scene Range	−20 °C to 150 °C (High Gain) −20 °C to 450 °C (Low Gain)
Digital Zoom	16 ×
Pixel Pitch	12 μm
Spectral Band	8–14 μm
Photo Format	R-JPEG
Video Format	MP4
Metering Method	Spot Meter, Area Measurement
FFC	Auto/Manual
Visual RGB Camera	
Sensor	1/2" CMOS, Effective Pixels: 48 M
Lens	FOV: 84° 35 mm format equivalent: 24 mm Aperture: f/2.8 Focus: 1 m to ∞
ISO Range	Video: 100–12800 (auto) Photos: 100–1600 (auto)
Digital Zoom	32 ×
Max Image Size	8000 × 6000
Still Photography Modes	Single shotInterval: 2/3/5/7/10/15/20/30/60 s Panorama: Sphere
Video Resolution	3840 × 2160@30fps 1920 × 1080@30fps
Photo Format	JPEG
Video Format	MP4

Source: https://enterprise.dji.com/mavic-2-enterprise-advanced/specs

Wirasatriya et al., 2019a; 2020; Setiawan et al.; 2019; 2020).

In the seas of Alor Kecil, Alor Island, Indonesia, there is an extreme upwelling event (EUE) that is characterized by a drastic SST drop reaching more than 10°C in a short time (Wirasatriya et al., 2023). Using continuous observation measurements, Wirasatriya et al. (2023) found the minimum SST due to EUE can reach 12°C, which makes this the only phenomenon in the world because none of the tropical areas has such cold SST. This phenomenon differs from the typical coastal upwelling in that it is tide-driven.

It only occurs monthly during spring tide for 1–3 days in August to November, twice a day following the local tidal type, with a duration of approximately 1 h in each event. EUE occurrence is also localized along the narrow strait, 300 m wide and 900 m long, called Mulut Kumbang Strait, separating Alor Kecil Village and Kepa Island (Fig. 1). During spring tide, flood (ebb) current brings the cold water entering (exiting) the strait (Wirasatriya et al., 2023).

Although the temporal distribution of EUE has been investigated by Wirasatriya et al. (2023), its spatial distribution remains unresolved. The medium resolution of satellite images with ~1–4 km spatial resolution, like the Advanced Very High-Resolution Radiometer (AVHRR) onboard the National Oceanic and Atmospheric Administration (NOAA) Satellite, Moderate Imaging Sensor (MODIS) onboard the Terra and Aqua satellites, and Geostationary Satellite Himawari, fails to capture the signal of EUE due to the small area coverage of EUE (Wirasatriya et al., 2023). High-resolution images like Landsat images also missed capturing the EUE due to low temporal resolution (i.e., 14 days). Even if the Landsat image's passing date is the same as the occurrence date of EUE, Wirasatriya et al. (2023) cannot capture the EUE due to the different acquisition timing between the satellite and EUE occurrence. Furthermore, the infrared radiometer onboard the satellite also has limitations in detecting SST in cloudy conditions. In the present status of satellite development, the detection of EUE using satellite measurement is impossible due to the absence of high spatial resolution of thermal infrared sensor onboard geostationary satellite that can observe at least hour by hour of SST fluctuation in a small-scale area.

In the present study, we provide aerial photos with the thermal infrared sensors mounted on the Unmanned Aerial Vehicle (UAV) during the EUE in the Mulut Kumbang Strait. Thus, this becomes the first study that reveals the spatial distribution of extremely cold SST, which is less than 15°C, in the tropics. Furthermore, the thermal aerial photos also managed to indicate the complex current pattern distribution during EUE.

2. Instruments and method

2.1. Instrument

The main instrument for investigating the spatial distribution of EUE in the seas of Alor Kecil is the thermal camera mounted on the DJI Mavic 2 Enterprise Advanced. The Mavic 2 Enterprise Advanced features a dual high-resolution RGB sensor and radiometric thermal camera system. The RGB camera was used to produce the high-resolution image for the base map. Table 1 present the detailed specifications of cameras mounted on the Mavic 2 Enterprise Advanced.

We deployed two temperature loggers, HOBO Pendant MX 2201, at 0.5 m depth attached at the floats for thermal camera validation. The

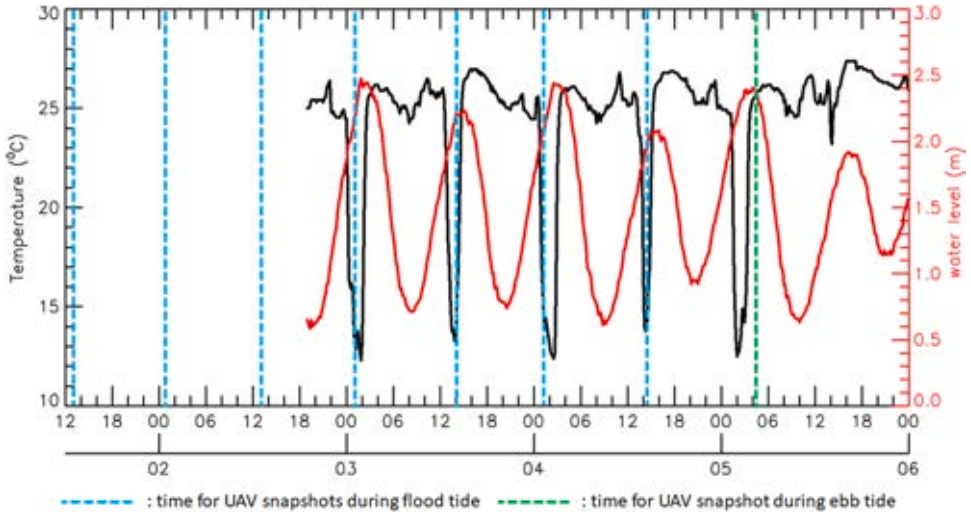

Fig. 2. Acquisition time of UAV images in September 2023 overlaid with temperature and tidal data obtained from HOBO U20L-01.

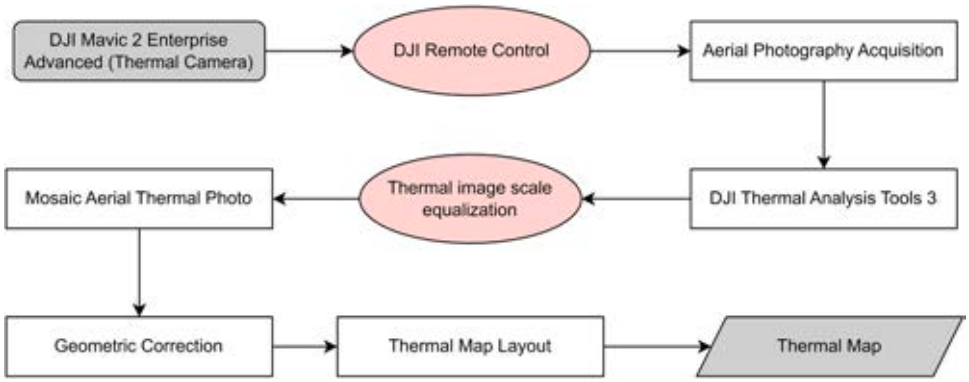

Fig. 3. Flowchart of thermal image acquisition and processing.

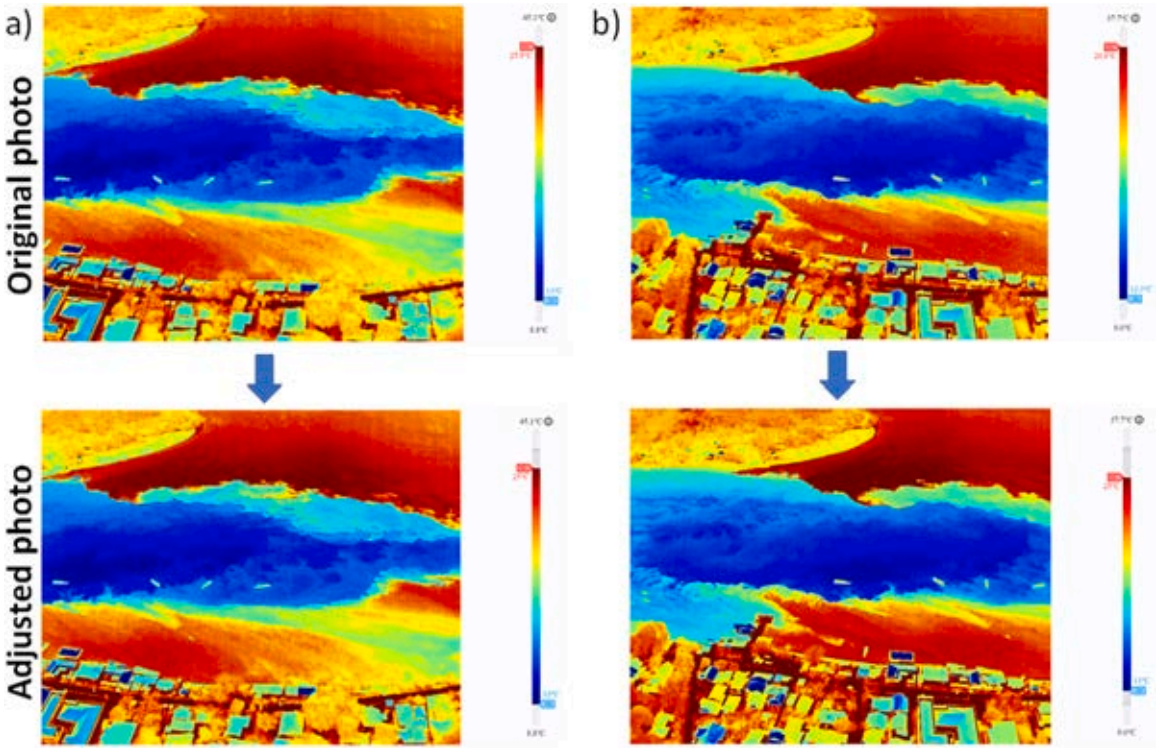

Fig. 4. Example of adjusting temperature scale of thermal photo using DJI Thermal Analysis Tool 3.

position of these temperature loggers can be seen in Fig. 1. Furthermore, water level logger HOBO U20L-01 was also deployed at Alor Kecil Pier (Fig. 1) to see the relationship between temperature and tide during EUE. We also use an upward-looking Teledyne RDI Workhorse Sentinel (WHS) 300 KHz Acoustic Doppler Current Profiler (ADCP) to get an idea of the current pattern during EUE. This is done at a depth of about 16 m and a measurement interval of 1 m in the Mulut Kumbang Strait (Fig. 1).

2.2. Method

For revealing the spatial distribution of EUE, we investigated the EUEs occurring on 1–5 September 2023, as shown in Fig. 2. Fig. 2 shows the acquisition time for UAV images overlaid with temperature and tidal data from the HOBO U20L-01 logger. Unfortunately, HOBO U20L-01 was deployed on 2 September 2023 at 19:00, thus there is no data before that. Overall, the temperature of nighttime EUE is lower than daytime EUE. The minimum temperatures during nighttime (daytime) EUE are around ~12°C (~13°C). The minimum temperature is 12.69 °C, occurred during nighttime on 4 September 2023 at 02:40 AM. We managed to capture 8 EUE cases; seven cases were taken during flood tide, and one case was taken during the beginning of the ebb tide that represent the peaks and the decay stages of EUE. Noting that, the time base presented in this paper is local time (WITA local time = UTC +8).

The procedures for thermal image acquisition and processing are schematically described in Fig. 3. First, we prepared the DJI Mavic 2 Enterprise Advanced flying route as shown in Fig. 1. Aerial photo acquisition was taken at 120 m height with manual flight operation and the oblique shooting method. The oblique shooting method was applied to save time with a wider scanning area to deal with the rapid changes of SSTs during EUEs. The acquisition process for all EUE cases used an intervalometer technique with an interval of 3 s. This method allows the UAV to take photos automatically every 3 s. It needed 10–15 min to capture the area along the Mulut Kumbang Strait during EUE.

The captured thermal aerial photos were automatically adjusted in the scale of temperature by the DJI Mavic 2 Enterprise Advanced, depending on the captured temperature objects, which made the temperature ranges different among photos. DJI Thermal Analysis Tool 3 software was used for all to synchronize the temperature ranges among

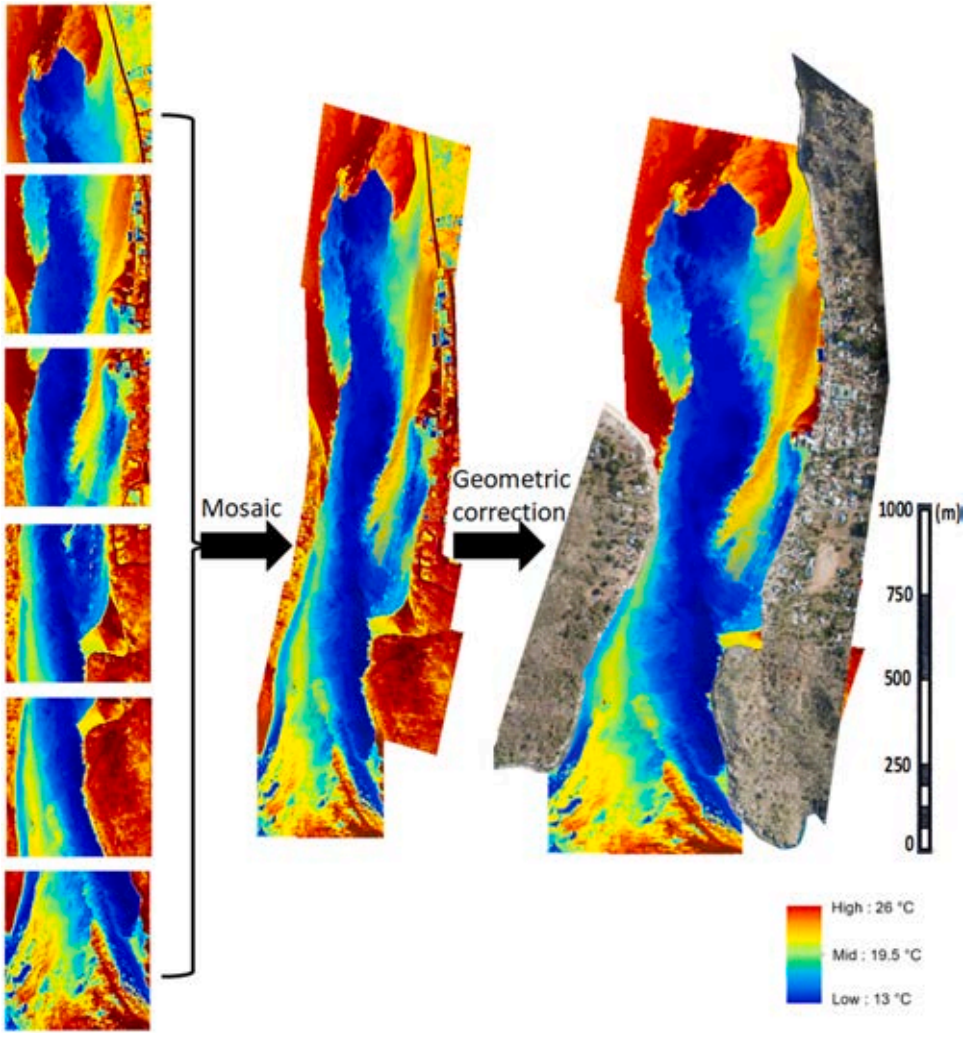

Fig. 5. Example of the mosaicking and geometric correction process of thermal photos on 4 September 2023.

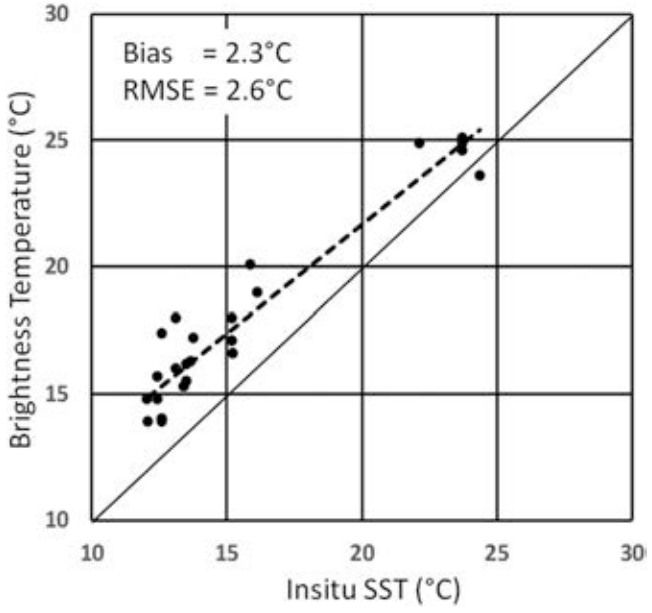

Fig. 6. Validation result of brightness temperature vs. in-situ SST. Dashed and solid lines denote the regression and y = x lines, respectively.

photos to make sure that all photos have the exact same temperature range. Fig. 4 shows an example of the adjusting process of the temperature scale. In the original photos, the temperature range of the left and right figures are 13°C - 25.9°C and 12.3°C - 26.6°C. Using DJI Thermal Analysis Tool 3, the temperature ranges for both images are adjusted into 13°C-25°C. All adjusted photos were then saved in JPEG format. This step is important before mosaicking thermal photos for each EUE event.

The mosaicking process of thermal photos data into a complete aerial photo image covering Mulut Kumbang Strait in one file was conducted by firstly selecting the photos. As seen in Fig. 5, we used only 6 thermal photos to construct a merged thermal photo of daytime EUE on 4 September 2023. The mosaicking process used Adobe Photoshop software with blending mode. This manual process was chosen because the automatic thermal orthomosaic process, as shown by Sedano-Cibrián et al. (2022), was not possible due to the complex SST pattern in the thermal photos. The mosaicked images were then exported in TIFF format for conducting geometric correction using ArcGIS 10.6 software. This process briefly provides coordinates for the photo that we have processed so that it has a geographical reference and it can be put precisely within the study area. The example of the mosaicking process until geometric correction is shown in Fig. 5. The final step was map layout by adding necessary map attributes to produce the thermal map for each EUE case in JPEG format. The final spatial resolution of the thermal map is 38 cm.

In addition, we also managed to take a video to record the decay

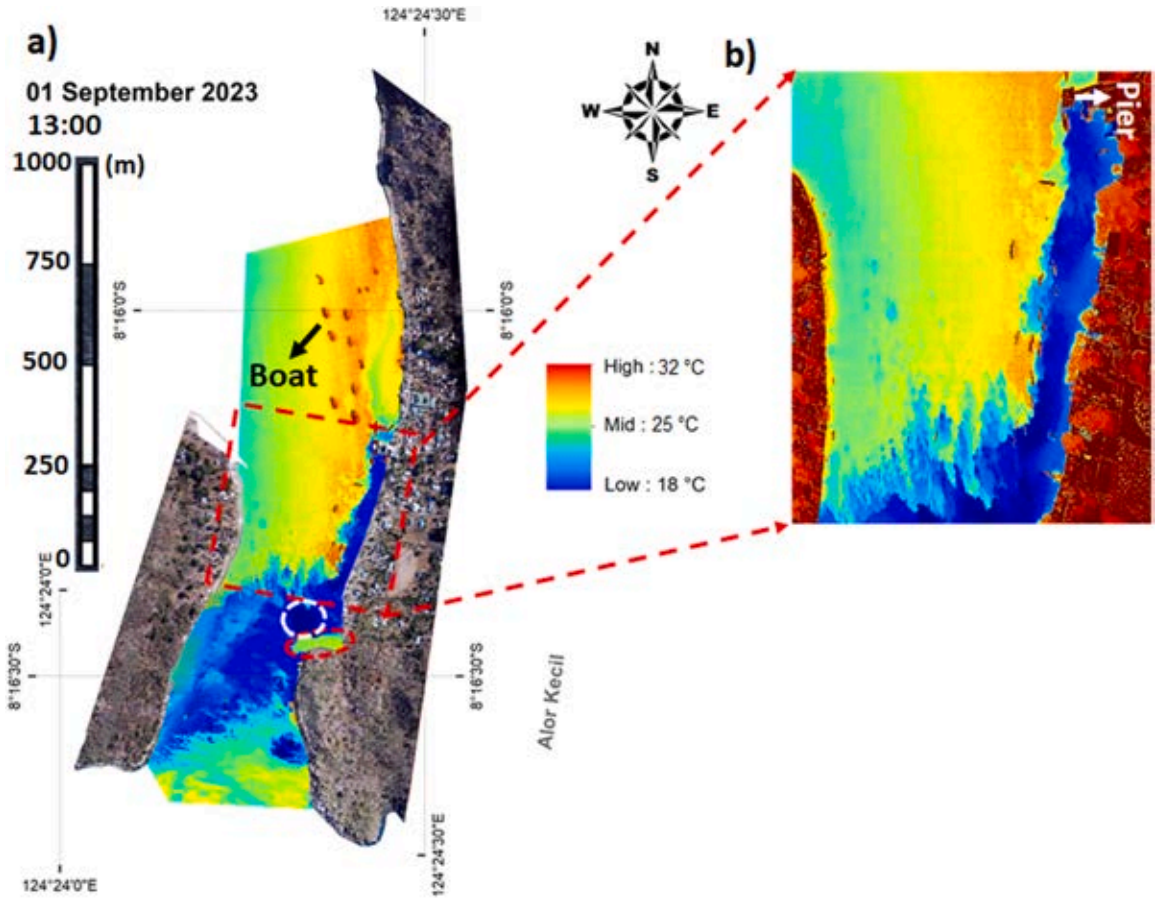

Fig. 7. Spatial distribution of BT during daytime EUE on 1 September 2023. White and red circles denote the position of the lowest temperature, i.e., 18°C, and the warm area inside the small bay, respectively.

process of EUE on 5 September 2023 at around 04:00. The video was taken at the mouth of Mulut Kumbang Strait at a fixed position. Considering the timing and distance of the southward propagation of the warm water, this video is helpful to estimate the propagation speed of warm water during the decay of EUE.

3. Result

3.1. Validation

Before conducting the analysis of the spatial distribution of EUE, the thermal photos obtained from DJI Mavic 2 Enterprise Advanced have been validated by in-situ measurements. The validation result is shown in Fig. 6. Since we did not perform any emissivity corrections, the thermal images collected by the UAV's infrared sensor are referred to as the brightness temperature (BT) instead of the actual SST. BT has a bias and root mean square error (RMSE) of 2.3°C and 2.6°C, respectively. Fig. 6 shows that BT has a systematic error to overestimate the in-situ SST by about 2.6°C. The error is smaller toward the higher temperature. Thus, since we use the original BT value sensed by the UAV sensor, the actual SST during the cold EUE may be lower than the BT as presented in this study. However, this accuracy is still acceptable since it matches with the accuracy provided by DJI factory, i.e., around 2°C, as shown in Table 1.

3.2. Spatial distribution of brightness temperature during the peak of EUE in the Seas of Alor Kecil

The spatial distribution of BT during the peak of EUEs is analyzed on daily basis from 1 to 4 September 2023 (Figs. 7–10). The first day of EUE in September 2023 occurred on 1 September 2023. However, our observation missed the nighttime EUE on September 1, 2023, at 01:00. The spatial distribution of daytime EUE on 1 September 2023 is presented in Fig. 7. The emergence of cold BT from the southern strait mouth to the north serves as a marker for the EUE occurrence.

However, since this is the first day of EUE, the minimum BT is only 18°C, which is denoted by a white circle. The warm water still dominates and occupies more than half of the strait. Nevertheless, cold water mass can penetrate further northward at the east side of the strait since the existence of a pier blocks the southward warm water movement (Fig. 7b). Red dots along the strait indicate the appearance of boats. The spatial distribution of BT on the first day of EUE indicates the existence of a northward flood current that pumps up and brings cold water mass entering the strait and the existence of a southward current that brings warm water mass to the strait. The confluence of both water masses creates a temperature front that clearly separates the warm and cold BT, Furthermore, Fig. 7 also shows that there is a sheltered area inside the small bay (red circle) that keeps the water warm.

The spatial distribution of BT in the second day of EUEs is presented in Fig. 8. EUEs have reached their peaks as denoted by the minimum temperatures that are less than 15°C. Minimum BT for nighttime and daytime EUEs are 12°C and 14°C, respectively. The northward advection of cold-water mass is clearly seen in both EUEs, which occupy almost all study areas. The penetration of cold-water mass mostly comes from the eastern side of the strait mouth. The small bay (red arrow in Fig. 7) still keeps the warm water mass, as also shown in the first day of EUE. Warm water plumes appear in the mouth strait for both cases, indicating that the northward flood currents entering the strait do not only bring the cold-water mass from the subsurface but also warm surface water from the southern Pantar Strait. The strong flood current

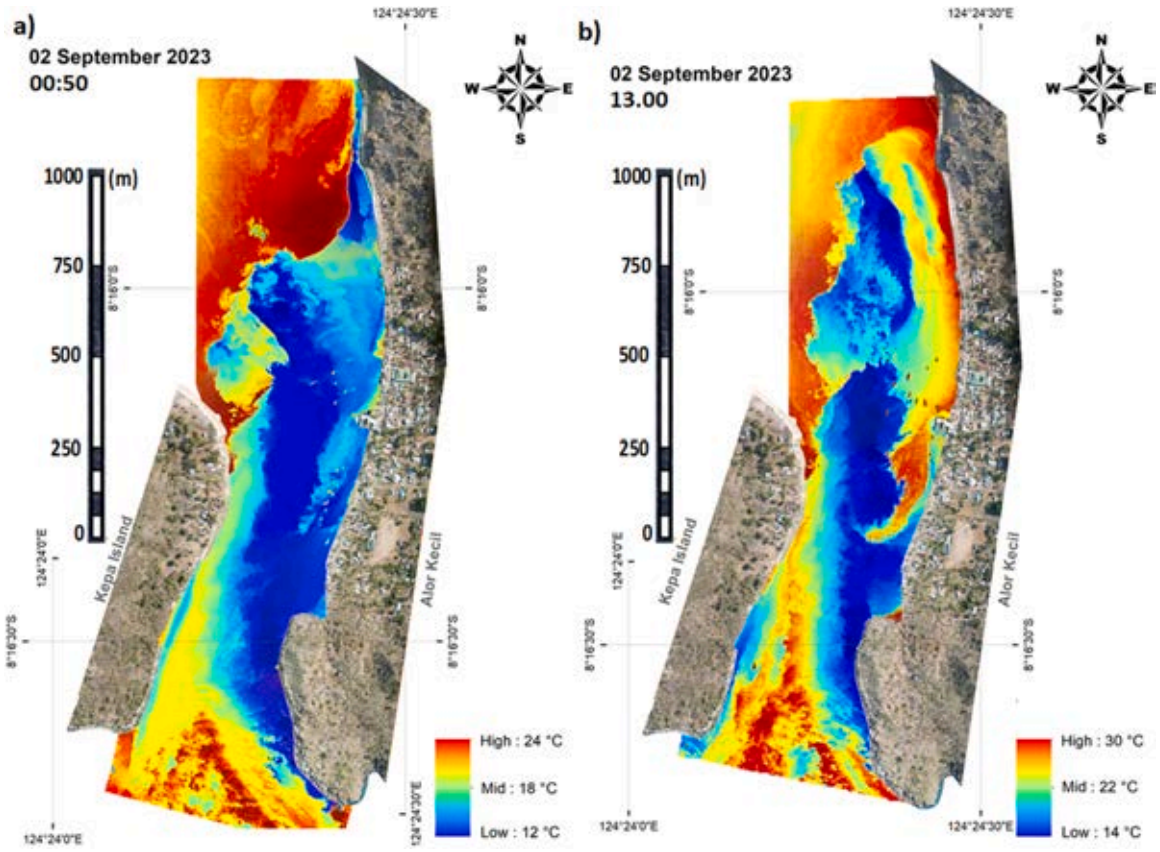

Fig. 8. Spatial distribution of BT during a) nighttime and b) daytime EUE on 2 September 2023.

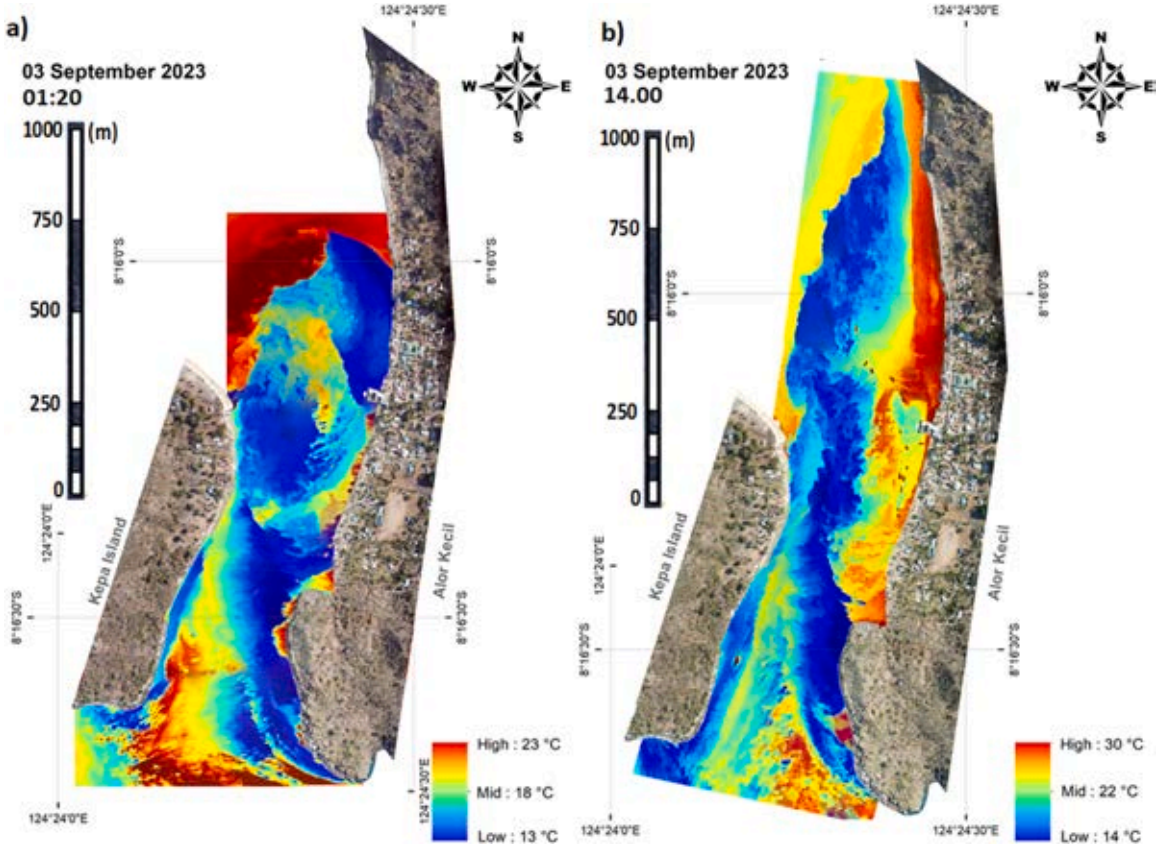

Fig. 9. Spatial distribution of BT during a) nighttime and b) daytime EUE on 3 September 2023.

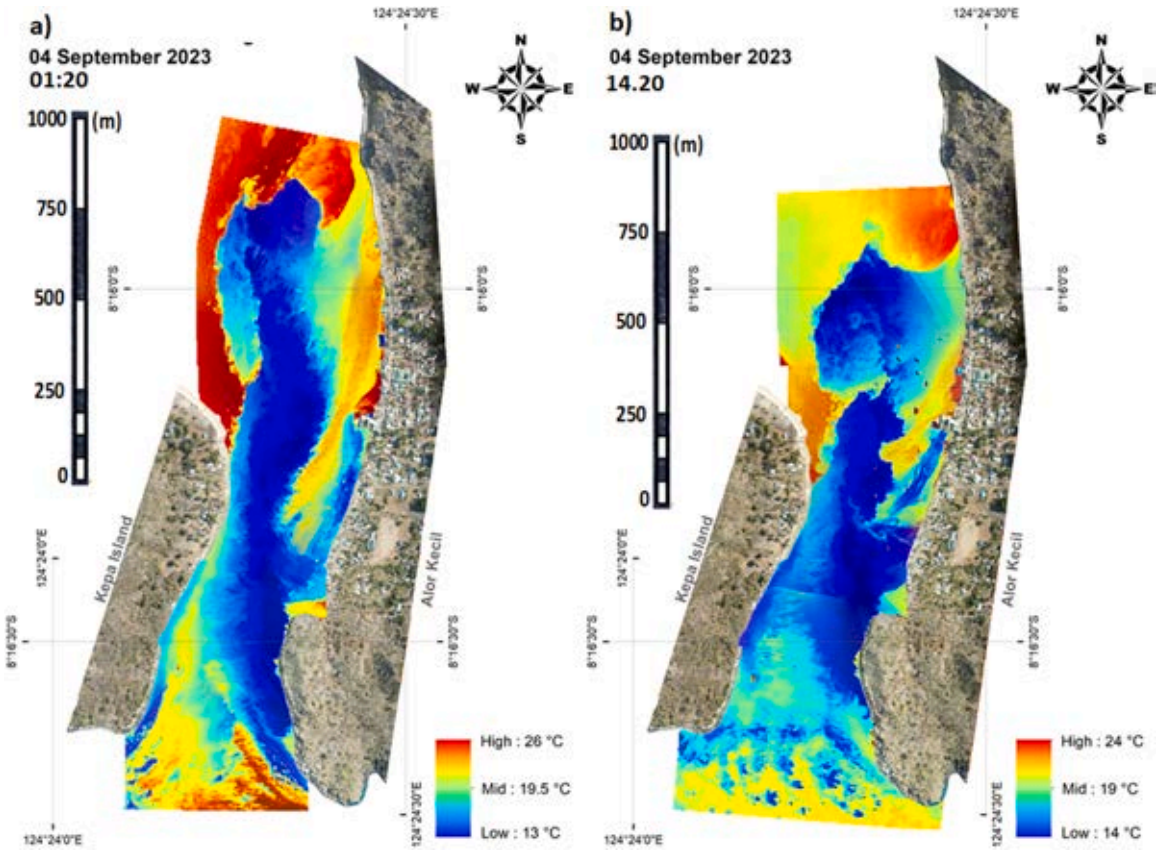

Fig. 10. Spatial distribution of BT during a) nighttime and b) daytime EUE on 4 September 2023.

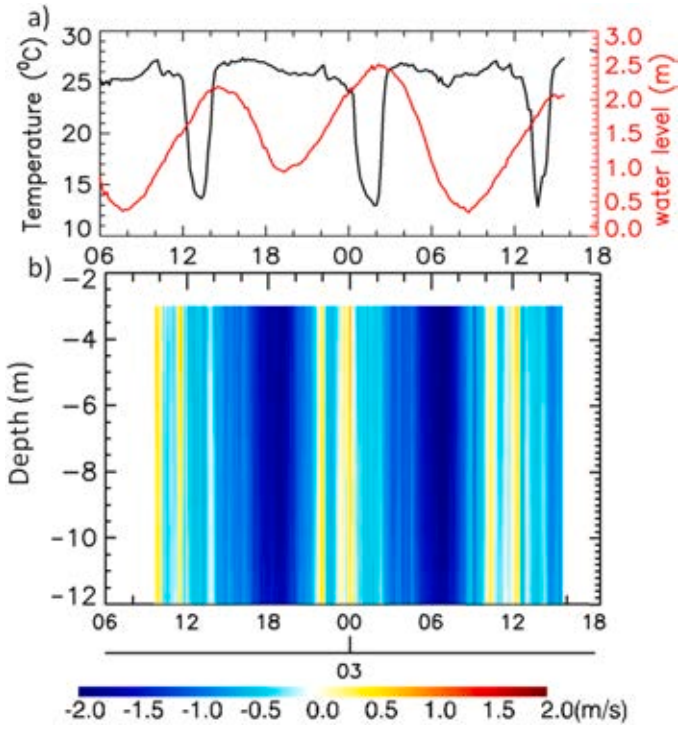

Fig. 11. a) Temperature and tidal data obtained from HOBO U20L-01 and b) Hovmoller diagram of the meridional component of current obtained from ADCP on 2–3 October 2023. Negative and positive values denote southward and northward currents, respectively. The position of HOBO U20L-01 and ADCP can be seen in Fig. 1.

pushes cold water mass around 1.5–2 km away from the strait mouth, replacing the warm water mass along the strait. This makes temperature fronts clearly seen at the northern part of the study area. Furthermore, the strong flood current forces the warm southward current to flow only along the northeastern fringe of the strait. Again, Alor Kecil Pier still plays a role in blocking and deflecting the warm southward current, creating a southward warm water tongue in both cases. With the temperature of 27°C, warm water tongue for daytime EUE is more obvious than nighttime EUE, which only reaches 16°C.

The spatial pattern of BT distribution of EUEs on 3 and 4 September 2023 (Figs. 9 and 10) is similar to EUE on 2 September 2023 (Fig. 8). Northward warm water plumes at the strait mouth exist for all cases. The nighttime EUEs have slightly lower minimum temperatures than daytime EUEs. This is probably due to the absence of solar heating during nighttime that makes the background temperature during nighttime lower than during daytime. Heat input from solar radiation increases SST during daytime (e.g., Ali, 1989; Alfarizi et al., 2023; Wirasatriya et al., 2019b). On the daytime of 4 September 2023, the northward warm water plume starts to fade, which indicates that the EUE has passed its peak. The mixing of warmer water plume and colder EUE water causes the background temperature during daytime on 4 September 2024 to be lower than the background temperature during nighttime.

The spatial distribution of all EUEs on 1–4 September 2023 confirms that the northward propagation of cold-water mass can reach 1.5–2 km away from the strait mouth, creating a strong BT front in the northern part of the strait. Comparing with bathymetry data in Fig. 1, the cold water propagation of all EUE cases follows a thalweg, the deepest path of channel in the Mulut Kumbang Strait, which is deeper than 20 m. This supports Wirasatriya et al. (2023) finding regarding the significance of bathymetry in the propagation of cold water mass. Fig. 7 of Wirasatriya et al. (2023) revealed the existence of a channel where the flood current

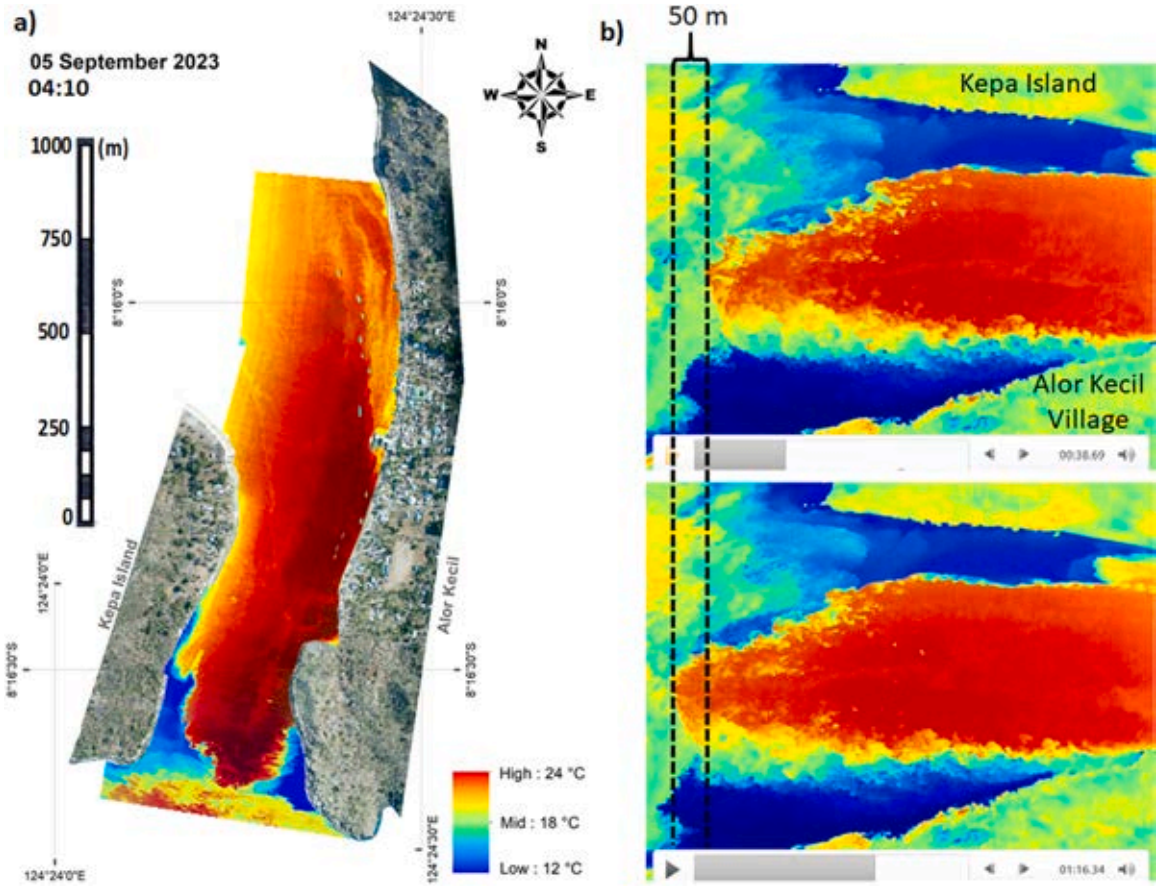

Fig. 12. a) Spatial distribution of SST and b) video analysis during the decay stage of nighttime EUE on 5 September 2023.

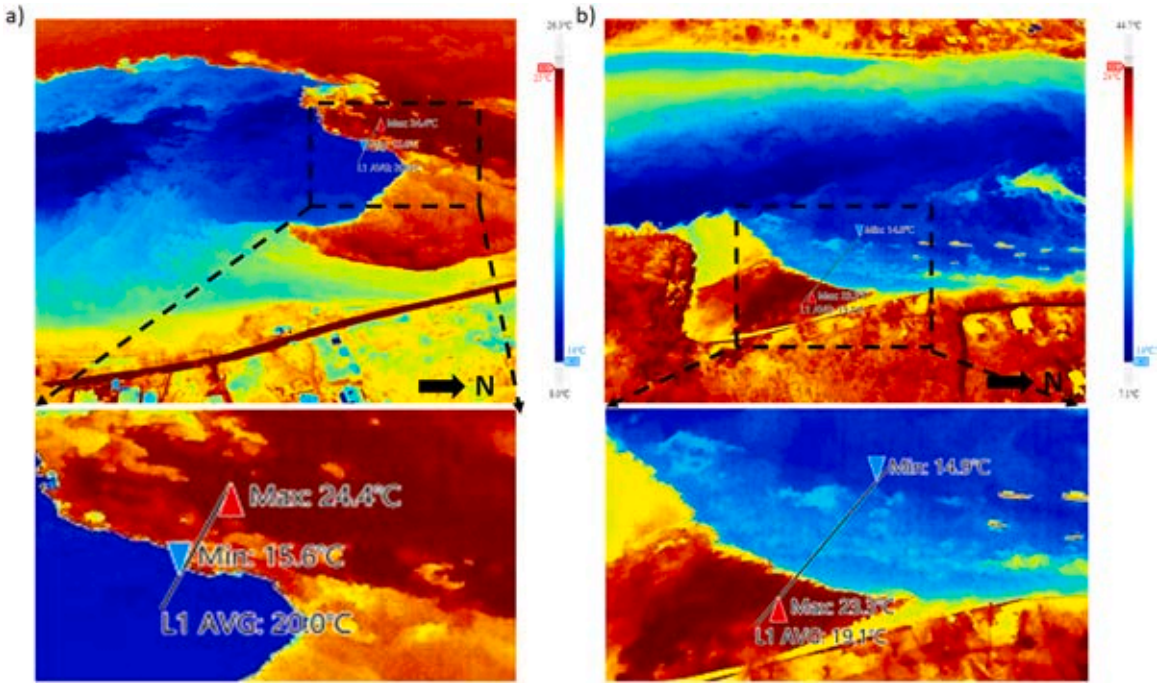

Fig. 13. Analysis of temperature difference along the training lines at a) the northern tip of EUE and b) the small bay as denoted by the red circle in Fig. 7a using DJI Thermal Analysis Tool 3.

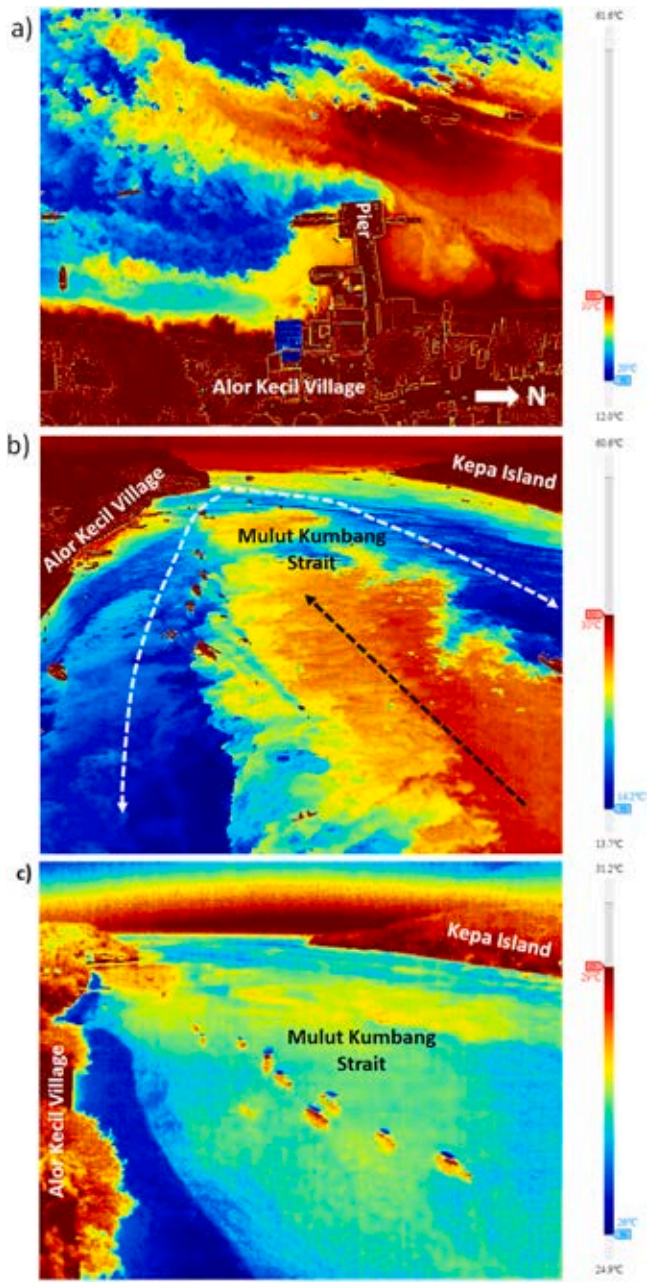

Fig. 14. a) The deflection of the southward warm water tongue due to the existence of a pier on 3 September 2023, 12:47, and b) Northward (white dashed lines) and southward (black dashed line) currents on 2 September 2023, 13:08, c) Brightness temperature distribution without EUE on 26 October 2022, 19:44, captured by a thermal camera onboard the UAV DJI Mavic 2 Enterprise Advanced.

during spring tide transports the cold water mass from the deep basin at the southern part of Alor Kecil waters directly to the Mulut Kumbang Strait following the thalweg. In addition, the appearance of warm water spots in the small bay (red circle in Fig. 7) is also detected in all cases with different magnitudes. The southward warm water tongues due to the deflection effect of the pier also appear in both daytime and nighttime EUEs.

To confirm the southward warm water tongue, we placed an ADCP on the path of this warm water tongue (Fig. 1) at ~16 m depth during EUE on 2–3 October 2023. Fig. 11 plots the meridional component of current at the path of the warm water tongue. It is clearly seen that the current profile is dominated by the southward current, both for the condition of flood and ebb tides. During ebb tide, the southward current speed ranges from 1 m/s to 2 m/s. During flood tide, northward currents are slightly detected among the weak southward currents. The weak southward currents are evident for the warm water tongue during EUEs. Furthermore, there is also no difference in current profiles among the depth layers, which indicates that the warm water tongue not only appears in the surface layer but also for the whole water column.

3.3. Spatial distribution of BT during the decay of EUE in the Seas of Alor Kecil

In the last day of EUE occurrence in the seas of Alor Kecil, we managed to capture the BT distribution during the decay of EUE in the beginning of the ebb tide (Fig. 12a). Strong southward ebb current brings the warm water, replacing the cold-water mass along the strait. Interestingly, despite the ebb current moving southward, the cold BT does not spread out off the strait mouth.

As a result, we can still make out the appearance of cold water surrounding warm water at the strait mouth's northern and southern sides. This indicates that the ebb current may push cold water mass back to the deeper water column through a channel in front of the strait mouth that is described by Wirasatriya et al. (2023). This fact emphasizes the crucial role of a channel as a path for cold water mass to transport from the deep basin to Mulut Kumbang Strait and vice versa.

Luckily, during the decay stage of EUE on 5 September 2023, we also managed to capture a video that can be used for estimating the propagation speed of the warm water. Fig. 12b shows the positions of the edge of warm water at 00:38.69 min and 01:16.34 min. With the distance between the edges of ~50 m and the duration of 37.65 s, the southward propagation of warm water mass is about 1.33 m/s. This value matches the speed of the ebb current measured by ADCP as shown in Fig. 11.

3.4. Discussion

The application of the UAV-mounted TIR sensors for the detection of cold water phenomena in the ocean was mostly conducted for investigating the characteristics of freshwater springs along the coastline (e.g., Lee et al., 2016; Oberle et al., 2022; Savonitto et al., 2022). They can detect the appearance of a freshwater plume off the spring from the indication of colder SST captured by the TIR sensor. In the present study, the spatial distribution of BT obtained from TIR sensors mounted on UAVs firstly reveals the detailed features of EUE in the seas of Alor Kecil during its peak and decay stages. We extended the findings in Wirasatriya et al. (2023), who indicate the only occurrence of EUE along the Mulut Kumbang Strait by using a limited number of temperature loggers, i.e., two units deployed inside and two units outside the strait. We found that the propagation of cold-water mass during the peak of EUE does not only spread along the Mulut Kumbang Strait but also reaches far to the north, up to 1 km from the tip end of the strait, where we can find the strong temperature front.

The appearance of a strong temperature front also becomes an interesting point that should be highlighted in the present study. SST front represents a boundary area between two stratified water masses in the ocean and coastal area (Belkin and Cornillon, 2003; Lin et al., 2019; Lukman et al., 2022; Ullman and Cornillon, 1999). It has a positive correlation with the occurrence of cooler SST at the coastal area, which is susceptible to upwelling, river runoff, and rainfall (Kahru et al., 2012; Olaya et al., 2021; Daulay et al., 2019; Lan et al., 2009). In the global ocean, the Kuroshio-Oyashio transition area becomes one of the areas with the existence of a strong SST front. Shimada et al. (2005) reported that the maximum magnitude of SST front in this area is around 0.3°C/km. At its southern part, the subtropical Pacific front also exists with the weaker magnitude, i.e., around 0.01°C/km (Qiu and Kawamura, 2012). Within the Indonesian Seas, Bahiyah et al. (2023) found that during the extreme positive IOD in 2019, a massive SST front anomaly was formed in the northern tip of Sumatra waters with the magnitude of 0.2°C/km. On a smaller scale, a strong SST front is found in

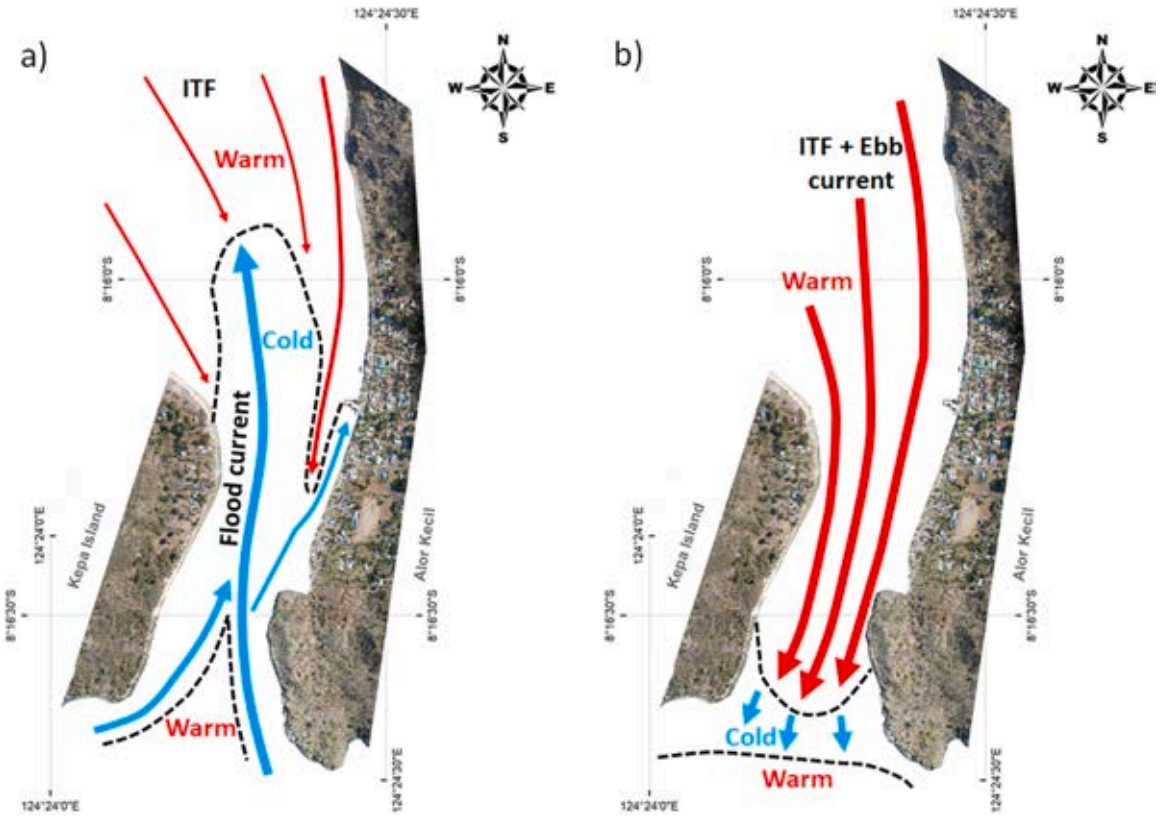

Fig. 15. Schematic figures of SST and current pattern during a) the peak and b) the decay of EUE in the seas of Alor Kecil. The dashed black lines denote SST fronts.

the Seto Inland Sea, Japan, during summer. With a width of about 5 km, SST changes by 2 °C in the Seto Inland Sea (Kida et al., 2015).

During the occurrence of EUE in the Mulut Kumbang Strait, it is easy to find the appearance of a strong SST front, as denoted by the temperature difference between 2 water masses, which can reach more than 5°C. Fig. 13 shows the example of maximum and minimum BT between the two water masses in the northern tip of EUE and in the small bay (red circle in Fig. 7a) during nighttime EUE on 4 September 2023. The maximum (minimum) temperature along the training line in the northern tip of EUE is 24.4°C (15.6°C). This means that the temperature difference between the two water masses is 8.8°C. In another case, the temperature difference between two water masses in the small bay is 8.4°C, with the maximum (minimum) temperature of 23.3°C (14.9°C). These temperature differences are not comparable with the SST front magnitude in the Kurosio-Oyasio transition area, the sub-tropical Pacific front, the tip of Sumatra Waters, and the Seto Inland Sea, Japan. Thus, the occurrence of extreme upwelling events in the seas of Alor Kecil forms an extreme SST front, which may become one of the strongest SST fronts in the world.

The detail BT feature presented in this study also reveals the complex current pattern during EUE. Based on the finding that changes in tide and temperature are related, Wirasatriya et al. (2023) said that flood tide (ebb tide) may bring in (bring out) the cold water mass through the process of tidal sloshing, which is the movement of water back and forth, during the growth (decay) of EUE. The present study managed to capture the spatial characteristics of flood and ebb currents during the peak and decay of EUE. The northward flood current clearly brings a cold water mass entering the strait, while the southward warm ebb current pushes back the cold-water mass to the deep layer in front of the strait mouth. One interesting feature found in this analysis is the southward current, which exists not only during ebb tide but also during the flood tide. This indicates that there is a background current that always flows southward in the seas of Alor Kecil. In the peak of EUE, the southward current creates a warm water tongue due to its interaction with the pier (Fig. 14a). Fig. 14b also shows the appearance of a warm southward current between the cold northward current at different angles. This southward current may correspond to the Indonesian Throughflow (ITF) that most of the time flows southward. In the normal condition, or without EUE occurrence, the cold northward current and warm southward current disappear, and the temperature along the strait is relatively uniform, ranging from 26°C to 28°C (Fig. 14c).

ITF is the only pathway for inter-ocean exchange in the tropics that connects the Pacific and Indian Oceans (i.e., Gordon and Fine, 1996). Regional and remote forcing from the Pacific and Indian Oceans, which create a pressure gradient as a result of the two oceans' different sea levels—higher in the Pacific and lower in the Indian Ocean—regulate the ITF (Wyrtki, 1987; Susanto and Song, 2015; Sprintall et al., 2019). There are three main exits of ITF before reaching the Indian Ocean, i.e., the Lombok Strait, the Ombai Strait, and the Timor Passage (see Fig. 1 for the location) (e.g., Gordon et al., 2010; Susanto et al., 2016; Sprintall et al., 2009). Recently, Susanto et al. (2021) found that the Alas Strait, which is located between Lombok Island and Sumbawa Island, serves a double role in the total ITF transport into the Indian Ocean: its southward flow enhances the total ITF during the boreal summer and reduces the total ITF during the boreal winter. The persistent southward current in the seas of Alor Kecil indicates that Mulut Kumbang Strait, or Pantar Strait in general, may also be one of the exit paths of ITF. The ITF flowing in the seas of Alor Kecil becomes the background current that always brings warm water mass during both flood and ebb tide conditions. During flood (ebb) tide conditions, tidal current flows northward against (southward in accordance with) the ITF. Thus, we hypothesize that for the generation of EUE in the seas of Alor Kecil, northward flood current should be strong enough to beat the southward ITF. This may also become the reason why EUE does not occur monthly. The physical mechanism of EUE can be further investigated by deploying long-term ADCP and conducting a numerical model simulation to find the clear relation between tidal current and baroclinic current, such as ITF (e.g., Yang et al., 2018, Cui et al., 2021) in the seas of Alor Kecil to prove this

hypothesis. This task is left for future study.

Lastly, we emphasize that through thermal infrared sensor mounted at UAV, we managed to reveal the spatial distribution of EUE in the seas of Alor Kecil. However, our results are mostly based on the descriptive analysis on the UAV imageries due to the software limitation of DJI thermal analysis tool 3 that only can process the thermal images in JPEG format. For future work, raster analysis should be performed to access pixel by pixel of brightness temperature value of EUE. Thus, the complex temperature pattern during EUE can be evaluated qualitatively using digital image processing and statistical analysis.

4. Conclusion

Aerial photos with the thermal infrared sensors mounted on the unmanned aerial vehicle reveals the spatial distribution of EUE in the seas of Alor Kecil. The detail feature of SST and current pattern during the peak and decay of EUE is summarized in schematic figure as shown in Fig. 15. During the peak of EUE, northward flood current brings cold water from the deeper layer in front of the strait mouth entering the strait and meets southward ITF, creating a strong SST front in the northern part of the strait. The flood current also brings the warm surface water from the Pantar Strait, forming the warm water plume among the cold-water masses inside the strait. In the northeastern part, a warm southward current penetrates far and creates a warm water tongue due to the deflection of a pier. During the decay of EUE, ebb current and ITF collide, creating a strong warm southward current that pushes the cold water back to the deep layer in front of the strait mouth. The spatial distribution of EUE as revealed by thermal infrared sensor mounted at UAV indicates the new insight of the interaction between the global scale circulation as represented by ITF and local scale tidal current that generate EUE in the seas of Alor Kecil, Alor Island, Indonesia.

Declaration of Competing Interest

The authors declare that they have no known competing financial interests or personal relationships that could have appeared to influence the work reported in this paper.

Acknowledgement

This research is supported by Universitas Diponegoro under the scheme of High Reputation of International Publication Research with grant number 185–98/UN7.D2/PP/V/2023. This work is also supported by the Physical Oceanography program of the U.S. National Aeronautics and Space Administration (NASA; grant #80NSSC23M0011) through Cooperative Earth System Sci Research Agreement and the National Science Foundation (NSF; grant #2242151) through the University of Maryland for R.D.S. We also thank to Adjunct Professor Program of Diponegoro University provided by World Class University Program, Indonesia Endowment Fund for Education, and the Hidro-Oceanographic Center, Indonesian Navy, for the Jala Citra 3 expedition that conducted a field survey in the seas of Alor Kecil. Special thanks to Bapak Rachmad Marweki and his family for their hospitality in providing the accommodation during the field survey.

Data availability

Data will be made available on request.

References

Alfarizi, H., Wirasatriya, A., Kunarso, K., Abdillah, M.R., Haryanti, D., 2023. Surface heat flux aspect on the variability of sea surface temperature and Chlorophyll-A along the Southern coast of java. Geogr. Tech. 18 (1), 134–148. https://doi.org/10.21163/Gt_2023.181.10.

Ali, M.M., 1989. Role of absorbed solar radiation on Indian Ocean surface temperature: a case study for calm winds using satellite data. Remote Sens. Environ. 30 (1), 107–111. https://doi.org/10.1016/0034-4257(89)90052-7.

Bahiyah, A., Wirasatriya, A., Mardiansyah, W., Iskandar, I., 2023. Massive SST-front anomaly in the tip of sumatra waters triggered by extreme positive IOD 2019 event. Int. J. Remote Sens. https://doi.org/10.1080/01431161.2023.2268821.

Belkin, I., Cornillon, P., 2003. SST fronts of the pacific coastal and marginal seas. Pac. Oceanogr. 1 (2), 90–113.

Cui, X., Yang, D., Sun, C., Feng, X., Gao, G., Xu, L., Yin, B., 2021. New insight into the onshore intrusion of the kuroshio into the east China Sea. J. Geophys. Res. Oceans 126, e2020JC016248. https://doi.org/10.1029/2020JC016248.

Daulay, S.R., Sari, T.E.Y., Usman, U., Jhonnerie, R., 2019. Characteristics of thermal front in the tropical waters of eastern Indian Ocean. J. Perikan. Univ. Gadjah Mada 21 (1), 25. https://doi.org/10.22146/jfs.39724.

Gordon, A.L., Fine, R.A., 1996. Pathways of water between the pacific and Indian oceans in the Indonesian seas. Nature 379 (6561), 146–149. https://doi.org/10.1038/379146a0.

Gordon, A.L., Sprintall, J., Van Aken, H.M., Susanto, R.D., Wijffels, S., Molcard, R., Ffield, A., Pranowo, W., Wirasantosa, S., 2010. The Indonesian throughflow during 2004–2006 as observed by the INSTANT program. Dyn. Atmospheres Oceans 50 (2), 115–128. https://doi.org/10.1016/j.dynatmoce.2009.12.002.

Kahru, M., di Lorenzo, E., Manzano-Sarabia, M., Mitchell, B.Greg, 2012. Spatial and temporal statistics of sea surface temperature and chlorophyll fronts in the california current. J. Plankton Res. 34 (9), 749–760. https://doi.org/10.1093/plankt/fbs010.

Kämpf, J., Chapman, P., 2016. The functioning of coastal upwelling systems. Upwelling Syst. World *31–65*. https://doi.org/10.1007/978-3-319-42524-5_2.

Kida, S., Mitsudera, H., Aoki, S., et al., 2015. Oceanic fronts and jets around Japan: a review. J. Oceanogr. 71, 469–497. https://doi.org/10.1007/s10872-015-0283-7.

Lan, K.W., Kawamura, H., Lee, M.A., Chang, Y., Chan, J.W., Liao, C.H., 2009. Summertime sea surface temperature fronts associated with upwelling around the Taiwan bank. Cont. Shelf Res. 29 (7), 903–910. https://doi.org/10.1016/j.csr.2009.01.015.

Lee, E., Yoon, H., Hyun, S.P., Burnett, W.C., Koh, D-C., Ha, K., Kim, D-J., Kim, Y., 2016. Unmanned aerial vehicles (UAVs)-based thermal infrared (TIR) mapping, a novel approach to assess groundwater dischargeinto the coastal zone. Limnol. Oceanogr.: Methods 14 (11), 725–735. https://doi.org/10.1002/lom3.10132.

Lin, L., Liu, D., Luo, C., Xie, L., 2019. Double fronts in the Yellow Sea in summertime identified using sea surface temperature data of multi-scale ultra-high resolution analysis. Cont. Shelf Res. 175, 76–86. https://doi.org/10.1016/j.csr.2019.02.004.

Lukman, A.A., Tarya, A., Pranowo, W.Setiyo, 2022. Surface thermal front persistence in malacca strait. J. Ilm. PLATAX 10 (2), 16. https://doi.org/10.35800/jip.v10i2.40879.

Oberle, F.K.J., Prouty, N.G., Swarzenski, P.W., et al., 2022. High-resolution observations of submarine groundwater discharge reveal the fine spatial and temporal scales of nutrient exposure on a coral reef: faga'alu, AS. Coral Reefs 41, 849–854. https://doi.org/10.1007/s00338-022-02245-8.

Olaya, F.C., Durazo, R., Oerder, V., Pallàs-Sanz, E., Bento, J.P., 2021. Ocean front detection with glider and Satellite-Derived sst data in the Southern california current system. Remote Sens. 13 (24), 5032. https://doi.org/10.3390/rs13245032.

Qiu, C., Kawamura, H., 2012. Study on SST front disappearance in the subtropical north pacific using microwave SST. J. Oceanogr. 69 (3), 417–426. https://doi.org/10.1007/s10872-012-0106-z.

Savonitto, G., Paganini, P., Pavan, A., Busetti, M., Giustiniani, M., Cin, M.D., Comici, C., Küchler, S., Gerin, R., 2022. Aerial drone imaging in alongshore marine ecosystems: Small-Scale detection of a coastal spring system in the North-Eastern adriatic sea. Remote Sens. 15 (19), 4864. https://doi.org/10.3390/rs15194864.

Sedano-Cibrián, J., Pérez-Álvarez, R., de Luis-Ruiz, J.M., Pereda-García, R., Salas-Menocal, B.R., 2022. Thermal water prospection with UAV, Low-Cost sensors and GIS. Application to the case of la hermida. Sensors 22 (18), 6756. https://doi.org/10.3390/s22186756.

Setiawan, R.Y., Setyobudi, E., Wirasatriya, A., Muttaqin, A.S., Maslukah, L., 2019. The influence of seasonal and interannual variability on surface Chlorophyll-a off the Western lesser sunda islands. IEEE J. Sel. Top. Appl. Earth Obs. Remote Sens. 12 (11), 4191–4197. https://doi.org/10.1109/JSTARS.2019.2948385.

Setiawan, R.Y., Wirasatriya, A., Hernawan, U., Leung, S., Iskandar, I., 2020. Spatio-temporal variability of surface chlorophyll-a in the halmahera sea and its relation to ENSO and the Indian Ocean dipole. Int. J. Remote Sens. 41 (1), 284–299. https://doi.org/10.1080/01431161.2019.1641244.

Shimada, T., Sakaida, F., Kawamura, H., Okumura, T., 2005. Application of an edge detection method to satellite images for distinguishing sea surface temperature fronts near the Japanese coast. Remote Sens. Environ. 98 (1), 21–34. https://doi.org/10.1016/j.rse.2005.05.018.

Sprintall, J., Gordon, A.L., Wijffels, S.E., Feng, M., Hu, S., Koch-Larrouy, A., Phillips, H., Nugroho, D., Napitu, A., Pujiana, K., et al., 2019. Detecting change in Indonesian seas. Front. Mar. Sci. 6, 257. https://doi.org/10.3389/fmars.2019.00257.

Sprintall, J., Wijffels, S.E., Molcard, R., Jaya, I., 2009. Direct estimates of the Indonesian throughflow entering the Indian Ocean: 2004–2006. J. Geophys. Res. 114 (C7). https://doi.org/10.1029/2008JC005257.

Susanto, R.D., Song, Y.T., 2015. Indonesian throughflow proxy from satellite altimeters and gravimeters. J. Geophys. Res. 120 (4), 2,844–2,855. https://doi.org/10.1002/2014JC010382.

Susanto, R.D., Waworuntu, J.M., Prayogo, W., Setianto, A., 2021. Moored observations of current and temperature in the alas strait: collected for submarine tailing placement, used for calculating the Indonesian throughflow. Oceanography 34 (1), 240–248. https://doi.org/10.5670/oceanog.2021.103.

Susanto, R.D., Wei, Z., Adi, T.R., Zheng, Q., Fang, G., Bin, F., Supangat, A., Agustiadi, T., Li, S., Trenggono, M., Setiawan, A., 2016. Oceanography surrounding krakatau volcano in the sunda strait, Indonesia, 264–172 Oceanography 29 (2). https://doi.org/10.5670/oceanog.2016.31.

Ullman, D.S., Cornillon, P.C., 1999. Satellite-Derived sea surface temperature fronts on the continental shelf off the northeast U.S. Coast. J. Geophys. Res. Oceans 104 (C10), 23459–23478. https://doi.org/10.1029/1999jc900133.

Wirasatriya, A., Setiawan, J.D., Sugianto, D.N., Rosyadi, I.A., Haryadi, H., Winarso, G., Setiawan, R.Y., Susanto, R.D., 2020. Ekman dynamics variability along the Southern coast of java revealed by satellite data. Int. J. Remote Sens. 41 (21), 8475–8496. https://doi.org/10.1080/01431161.2020.1797215.

Wirasatriya, A., Sugianto, D.N., Helmi, M., Maslukah, L., Widiyandono, R.T., Herawati, V.E., Subardjo, P., Handoyo, G., Haryadi, Marwoto, J., Suryoputro, A.A. D., Atmodjo, W., Setiyono, H., 2019b. Heat flux aspects on the seasonal variability of sea surface temperature in the java sea. Ecol. Environ. Coserv. 2 (1), 434–442.

Wirasatriya, A., Sugianto, D.N., Helmi, M., Setiawan, R.Y., Koch, M., 2019a. Distinct characteristics of SST variabilities in the sulawesi sea and the Northern part of the maluku sea during the southeast monsoon. IEEE J. Sel. Top. Appl. Earth Obs. Remote Sens. 12 (6), 1763–1770.

Wirasatriya, A., Susanto, R.D., Kunarso, K., Jalil, A.R., Ramdani, F., Puryajati, A.D., 2021. Northwest monsoon upwelling within the Indonesian seas. Int. J. Remote Sens. 42 (14), 5437–5458. https://doi.org/10.1080/01431161.2021.1918790.

Wirasatriya, A., Susanto, R.D., Setiawan, J.D., Agustiadi, T., Iskandar, I., Ismanto, A., Nugraha, A.L., Puryajati, A.D., Kunarso, Purwandana, A., Ramdani, F., Lestari, T.A., Maro, J.F., Kitarake, Y.N.S., Sailana, Y.L., Goro, M.S., Hidayah, B.K., Widiaratih, R., Fitria, S., Dollu, E.A., 2023. Extreme upwelling events in the seas of the alor kecil, alor island, Indonesia, 3 – 0 Oceanography 36 (1). https://doi.org/10.5670/oceanog.2023.107.

Wyrtki, K., 1987. Indonesian through flow and the associated pressure gradient. J. Geophys. Res. 92 (C12), 12,942–12,946. https://doi.org/10.1029/JC092iC12p12941.

Yang, D., Yin, B., Chai, F., Feng, X., Xue, H., Gao, G., Yu, F., 2018. The onshore intrusion of kuroshio subsurface water from February to July and a mechanism for the intrusion variation. Prog. Oceanogr. 167, 97–115. https://doi.org/10.1016/j.pocean.2018.08.004.